Influence of Te impurity on morphology of GaSb epilayer grown on GaSb (001) patterned substrate by liquid phase epitaxy

G. Zhang, P. Jayavel, T. Koyama, M. Kumagawa, and Y. Hayakawa[a)]
Research Institute of Electronics, Shizuoka University, 3-5-1 Johoku, Hamamatsu, Shizuoka 432-8011, Japan

(Received 18 May 2004; accepted 25 October 2004; published online 27 December 2004)

We have studied the effect of Tellurium (Te) impurity on morphology of GaSb epilayer grown on GaSb (001) circular patterned substrates by liquid phase epitaxy. The results of the Te doped GaSb epilayers have been compared with the undoped GaSb epilayer under identical growth conditions. After the addition of Te impurity up to 0.12 mol % in the starting solution, it is observed that a (311)B facet is formed instead of a (111)B facet while there is no such transition in the (111)A facet. The reason for the transition of the (111)B facet to the (311)B is discussed and an atomic model is proposed to explain the transition of the facet. The cross-sectional (110) plane of the Te doped GaSb epilayer after stain etching in a permanganate etchant reveals that two boundaries are separating differently doped upper and lateral regions of the epilayer. Furthermore, a few Te impurity striations are observed in the lateral region of the epilayer but none are found in the upper region. The growth time dependence of the morphology of Te doped GaSb epilayer shows that the (311)B facet is initially formed and becomes dominant after three hours growth. © *2005 American Institute of Physics*. [DOI: 10.1063/1.1834723]

I. INTRODUCTION

In recent years, the growth of epilayers with pyramidal structure has attracted much attention because of their promising potential applications to optical devices.[1–6] Campbell and Green found that pyramidal texturing of the substrate surface gave rise to a significant degree of light trapping within the substrate.[1] Based on the pyramidal textured structure, silicon solar cell with a high efficiency was obtained.[2,3] Furthermore, a silicon light emitting diode (LED) with pyramidal textured structure has an efficiency of 1%, which is about 100 times higher than the previous silicon LED.[4] Williams *et al.* have reported that the square based pyramidal structures have the desired geometry for the formation of a corner cube mirror upper reflector and for microcavity device applications by regrowth.[6] Compared with vapor phase epitaxy, liquid phase epitaxy (LPE) has the advantage of offering higher crystal quality as well as greater selectivity in selective area epitaxy. For the past few years, GaSb has been considered as a promising material for detectors, thermophoto voltaic (TPV) cells, etc., in the near infrared region.[7] In our previous investigations, a hollow truncated pyramidal structured GaSb epilayer was grown on a GaSb (001) patterned substrate.[8] It has been shown that the pyramidal epilayer can be employed to fabricate a TPV cell. Further, an efficient light trapping has been expected in the pyramidal epilayers and subsequently to improve the conversion efficiency of the TPV cells.

In this work, we have investigated the influence of *n*-type dopant (Te) on the morphology of GaSb epilayer grown on GaSb (001) circular patterned substrates by LPE. The growth time dependence of the morphology on the Te doped GaSb epilayer has also been studied.

II. EXPERIMENT

In this study, GaSb (001) patterned substrates with a circular open window diameter of 600 μm were used. Figure 1 shows the schematic illustration of the patterned substrate. In order to fabricate the patterned substrate, first a 0.2 μm thick amorphous SiN_x film was deposited on GaSb (001) substrates by plasma assisted chemical vapor deposition using SiH_4 and N_2 gases. The circular open windows in the SiN_x film were formed by the combination of standard photolithography and reactive ion etching using CF_4 and O_2 gases.

A conventional LPE system was employed to grow the epilayers on the patterned substrates. After loading the source materials of 6 N Ga, undoped polycrystalline GaSb and Te polycrystalline powder (for Te doped GaSb epilayer), a graphite boat was heated to 700 °C and held at the temperature for 3 h to make the solution homogeneous. Subsequently, the solution was cooled down to 550 °C and kept in contact with an undoped GaSb source substrate for an hour to saturate the solution. Epitaxial growth was carried out with a supercooling of 1 °C by decreasing the temperature from 549 °C at a cooling rate of 10 °C/h. The residual so-

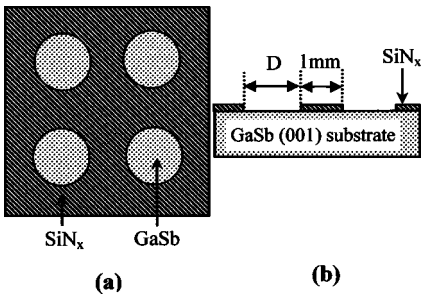

FIG. 1. Schematic illustrations of a GaSb (001) substrate with circular open seed window, (a) top view, and (b) cross-sectional view.

[a)]Corresponding author; electronic mail: royhaya@ipc.shizuoka.ac.jp

lution on the epilayer surface was removed by immersing the samples in a dilute HCl solution. The resulting epilayers were analyzed by a scanning electron microscope (SEM) facility. All the SEM images were recorded under secondary electron mode. The cross section of the Te doped GaSb epilayer was analyzed after stain etching in a permanganate etchant.

III. RESULTS AND DISCUSSION

A. Influence of Te doping concentration on morphology of GaSb epilayer

In order to analyze the effect of Te doping concentration on the morphology of a GaSb epilayer, undoped GaSb and Te doped GaSb epilayers have been grown on GaSb (001) substrate with circular open seed window under the identical growth conditions. The corresponding SEM images of the epilayers are shown in Fig. 2(a), undoped GaSb and Te doped GaSb epilayers with Te concentration in the starting solution of (b) 0.012 mol %, (c) 0.053 mol %, and (d) 0.12 mol %. It is observed that the undoped GaSb epilayer shows a hollow truncated pyramidal structure with mirrorlike top (001) and side {111} facets. In our previous work, the side {111} facets of the pyramidal epilayers have been identified as two kinds of facets, namely, (111)A and (111)B.[8] In contrast, Te doped GaSb (hereafter, GaSb:Te) epilayers show a complicated polyhedron structure. Figures 2(b) and 2(c) show the GaSb:Te epilayers, which appear as a hollow truncated polyhedron structure with top (001) facet and irregular side faces. The epilayer shown in Fig. 2(d) is a regular polyhedron structure with regular side faces and without a top (001) facet. It is clearly seen that the morphology of the undoped GaSb epilayer is dramatically modified due to the addition of Te impurity.

The structure of the Te doped GaSb epilayer as shown in Fig. 2(d) is explained as follows: the GaSb:Te sample is cleaved to reveal the (110) cross-sectional plane and then lapped down up to the line W-W′ as drawn in Fig. 2(d), subsequently polished with an alumina powder of average grain size of 0.05 μm. In order to reveal Te impurity distribution on the (110) cross-sectional plane, a permanganate etchant ($KMnO_4$(0.05M):HF:CH_3COOH=1:1:1, vol. ratio) is used to etch the sample since the etchant is shown to be very sensitive to reveal the Te striations in InSb and InGaSb crystals.[9,10] The etching was carried out at room temperature for 5 min. The resulting SEM image is shown in Fig. 3(a), in which the angle between the side facets and (001) substrate surface is found to be 25.2°. Thus, the two side facets are identified as (311)B. The other two side facets are identified as (111)A according to a inverse triangular etch pattern as shown in the inset of Fig. 3(a), which is a surface feature of the (111)A surface.[8] The irregular side faces of the GaSb:Te epilayers in Figs. 2(b) and 2(c) become a regular face, (311)B facet [Fig. 2(d)] with increasing the Te concentration in the starting solution. In addition, the growth in the central seed area of the substrate is completed so that the hollow structure is not observed for highly Te doped epilayers, as shown in Figs. 2(d) and 3(a).

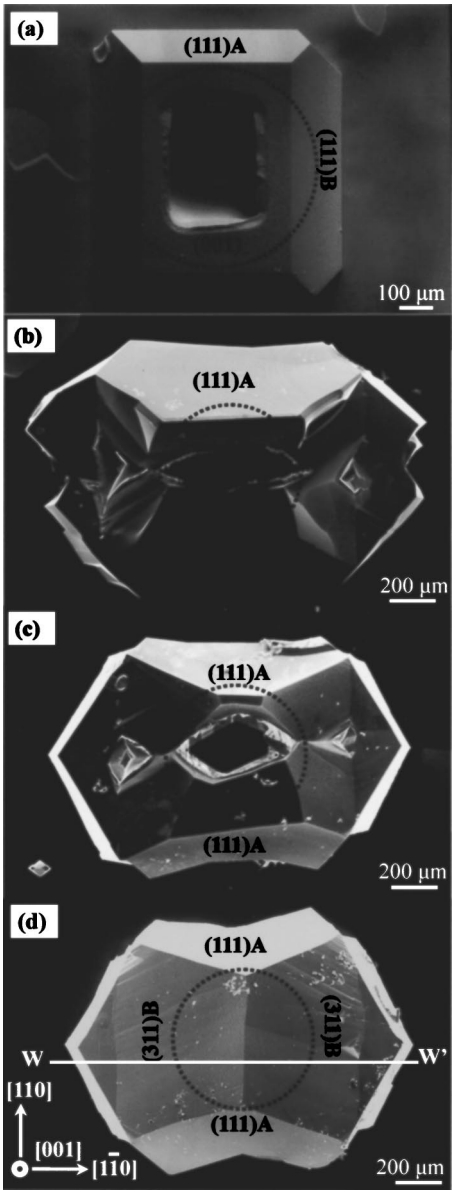

FIG. 2. SEM images of (a) undoped GaSb and Te doped GaSb epilayers with Te concentration in the starting solution of (b) 0.012 mol %, (c) 0.053 mol % and, (d) 0.12 mol %. Dashed circle represents the edge of the circular open seed window.

Since the lateral growth is an anisotropic growth of various crystal faces, the growth rate depends on the stability of the crystal face. If the growth rate is low, the crystal face has higher stability. For the undoped GaSb epilayer, the (111)B facet has the lowest growth rate. After the addition of Te impurity, the (111)B facet is modified to (311)B facet. The observed result indicates that the (311)B facet becomes more stable than the (111)B facet after the addition of Te impurity. Similar results have been observed by the doping of Te impurity into GaInP and GaAs epilayers grown by organometallic vapor phase epitaxy.[11,12]

Two possible origins for the transition of (111)B facet to (311)B can be considered; first, the facet transition depends on the number of available bonds to the Te atom on the surface. A Sb atom on the (111)B surface may bond to three underlying Ga atoms. The remaining bond in the tetrahedral

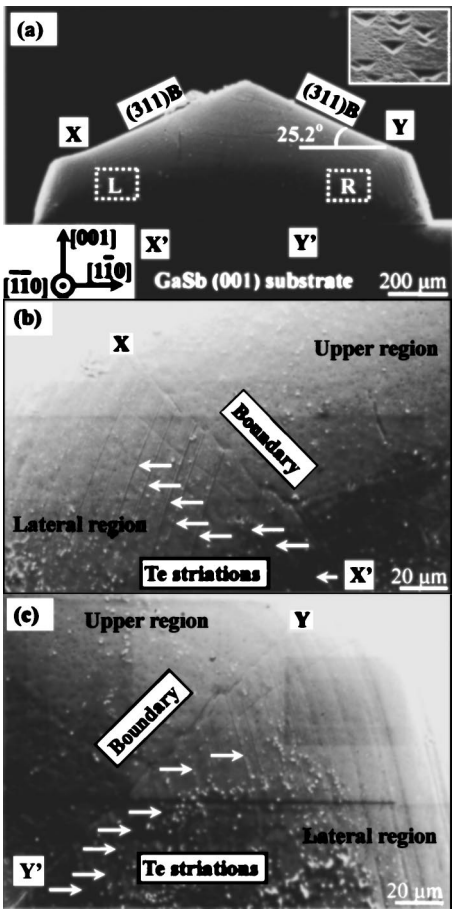

FIG. 3. (a) Cross-sectional image of Te doped GaSb epilayer along the line W-W′, as shown in Fig. 2(d) after stain etching. The inset shows an etch pattern on the (111)A facet after etching in $HCl:HNO_3:H_2O=1:1:1$, vol. ratio for 3 min at room temperature. (b) and (c) are the magnified images of the dashed regions *L* and *R* drawn in (a), respectively.

configuration of the Sb bonds either to another Sb atom forming a dimer or surface reconstruction of the (111) B. However, Te has more electrons in the outer bonding shell and so will not form the same dimer or surface reconstruction as Sb atom. Lee and Stringfellow have reported that the value of *n* with only odd values for the (11*n*) facets inside the surface step increases with increasing Te doping concentration in GaAs.[12] Second, III–V compound semiconductors with zinc blende structure exhibit different polarities along ⟨111⟩ directions. The outermost atomic layer in each face is composed of either group III [for (111)A face] or group V [for (111)B face] atoms which are triply bonded to the lattice. Furthermore, each (111)B surface atom has one dangling single bond whereas each (100) surface atom has one dangling double bond. On the other hand, (211)B, (311)B, and (511)B surfaces are composed of dangling single and double bond sites, which make the surfaces partially (111)-like and partially (100)-like. In the case of (311)B surface (see Fig. 4), there are equal densities of dangling single and double bond sites resulting in equal weighting of the (111)-like and (100)-like components.[13] Based on the discussions, an atomic model is proposed to explain the transition of the (111)B facet to the (311)B facet. It is known that the Te atom occupies Sb site and forms antisite complexes ($V_{Ga}Ga_{Sb}Te_{Sb}$)

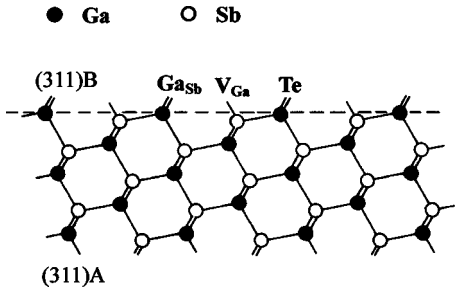

FIG. 4. Schematic diagram of antisite complexes ($V_{Ga}Ga_{Sb}Te_{Sb}$) formed on the (311)B surface.

for GaSb:Te epilayer grown by liquid phase epitaxy.[14,15] In Fig. 4, the dangling bonds on the (311)B surface can provide three adjacent dangling bonds to form the antisite complexes ($V_{Ga}Ga_{Sb}Te_{Sb}$), while there is no such surface structure on the (111)B surface. As a result, the antisite complexes could preferentially occur on the (311)B surface, and therefore, the (311)B facet is stabilized.

On the other hand, the reason for the unmodified (111)A facet can be explained as follows: For GaSb:Te epilayer, the outermost atomic layer in the (111)B face is composed of Te, Ga, and Sb atoms, while the outermost atomic layer in the (111)A face is composed of only Ga atom. Thus, the atomic structure of the (111)A facet is unmodified in contrast to the (111)B facet, which is reconstructed to the (311)B facet after the addition of Te impurity up to 0.12 mol % in the starting solution. However, further investigations are necessary to correlate the reconstructions of the (111)B and (311)B surfaces.

B. Formation of boundaries and striations in GaSb:Te epilayer

Figures 3(b) and 3(c) show the magnified SEM images of the dashed regions *L* and *R* drawn in Fig. 3(a), respectively. It is observed that there are two zigzag boundaries (*XX′* and *YY′*) and a few striations under the zigzag boundaries, as indicated by white arrows in Figs. 3(b) and 3(c). Indeed, the two zigzag boundaries originate from the interface of SiN_x mask layer (*X′*, *Y′*) and propagate into the surface of the epilayer (*X* and *Y*). The corresponding two regions separated by the boundary are assigned as the upper and lateral regions, as shown in the Figs. 3(b) and 3(c), respectively. Since the stain etchant is very sensitive to Te distribution,[9,10,16] the observed result implies that the striations are composed of Te. It should be noted that no such Te striations found in the upper region, as indicated in Fig. 5.

It is well known that the Epitaxial Lateral Overgrowth (ELO) layer has different properties of the upper and lateral regions.[16] Zytkiewicz *et al*. have found that differently doped regions of the GaAs:Te layer were separated by two boundaries and the upper region of the epilayer showed increased cathodoluminescence intensity.[17] Zhang *et al.* have also observed the similar result for a nitrogen doped GaP ELO layer.[18] In our case, the formation of the boundaries is due to different growth mechanisms between the upper and lateral regions. Since the striations in the lateral region are originated from the solid–liquid interface during the growth, it is

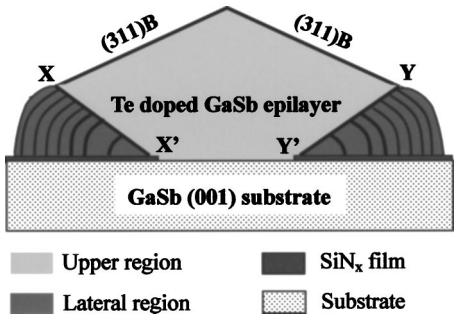

FIG. 5. Schematic diagram of cross-sectional view of the GaSb:Te epilayer, as shown in Fig. 3(a).

believed that the lateral growth front is atomically rough face, and the atoms can be added in a random fashion. On the other hand, the upper region with a growth front of the (311)B facet grows by two-dimensional nucleation or propagation of steps through substrate dislocations. As a consequence, two different incorporation rates of impurity on the regions could be expected. On the rough lateral growth front, the Te impurity distribution coefficient should be the equilibrium one, but on the upper singular face, the kinetics should govern the impurity incorporation process with the distribution coefficient being dependent on the vertical growth rate. As a result of the different incorporation rates of the impurity, Te striations occur in the lateral region but none are found in the upper region. Witt *et al.* have reported that the impurity striations are due to variations of nonequilibrium distribution coefficients, which are caused by temperature fluctuations near the solid–liquid interface.[19] These Te striations are equally likely to appear in both the lateral region and the upper region. However, our results show that the striations occur only in the lateral region. This is direct evidence to highly support that there are different mechanisms of incorporation of Te atoms in the upper and lateral regions.

C. Effect of growth time on morphology of GaSb:Te epilayer

The time dependence of the growth morphology of the GaSb:Te epilayer is studied in order to investigate the formation process of the (311)B facet. Figures 6(a) and 6(b) show the GaSb:Te epilayers with the Te concentration in the starting solution of 0.12 mol % for the growth time of 30 and 60 min, respectively. It is found that the (311)B facet is formed initially [Fig. 6(a)], and then develops gradually [Fig. 6(b)] and becomes dominant after 3 h growth, as shown in Fig. 2(d). The boundaries between the upper region and the lateral region can be observed in different periods on the surface of the epilayers, as shown in Figs. 6(a) and 6(b). In addition, the lateral growth front face along the [1–10] orientation appears as a zigzag line, which contains many growth front faces. These growth front faces coalesce with additional growth, as indicated by the white dashed arrows.

Figure 7(a) shows the cross-sectional (1–10) plane view of the epilayer, as shown in Fig. 6(b) after stain etching using the same conditions as described in Sec. III A. The corresponding cross-sectional schematic illustration is shown in Fig. 7(b). As can be seen in Fig. 7(a), two downward facets

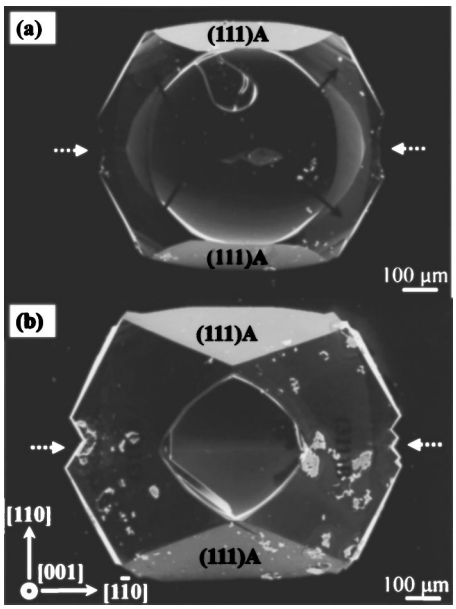

FIG. 6. SEM images of the GaSb:Te epilayers with Te concentration of 0.12 mol % in the starting solution for growth time of (a) 30 min and (b) 1 h. The lateral growth fronts are indicated by the dashed white arrows.

are formed under two (111)A facets and they are identified as (311)B facets since the angle between the downward facet and (001) substrate surface is about 72.5°. It should be noticed that the growth front in the [110] direction is different from that in the [1–10] direction, which is atomically rough as shown in Fig. 3(a). Indeed, the growth front face in this direction is initially faceted and there is no Te striations found in the lateral region along the [110] direction. The observed result agrees well with the results presented in Sec. III B. Since the (111)A and (311)B facets grow as the side facets of the GaSb:Te epilayer, the two faces are relatively stable compared with all the other crystal faces.

IV. CONCLUSION

In summary, we have investigated the influence of Te impurity on the morphology of GaSb pyramidal epilayer

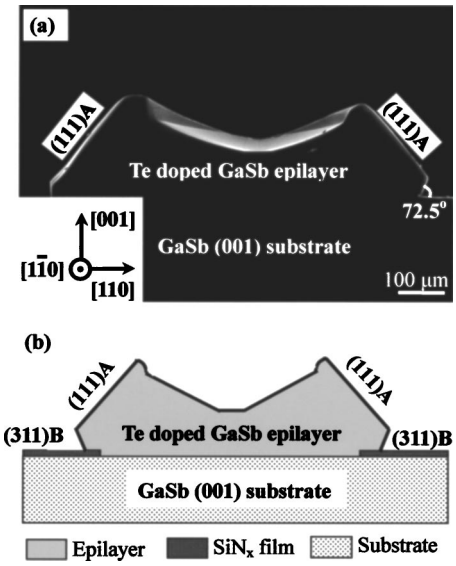

FIG. 7. (a) Cross-sectional view of the GaSb:Te epilayer as shown in Fig. 5(b) after stain etching. (b) Schematic illustration of the cross section.

grown on GaSb (001) circular patterned substrates. A transition of the (111)B facet to the stable (311)B facet is observed, while there is no such transition in the (111)A facet with increasing Te concentration in the starting solution up to 0.12 mol %. On the basis of the proposed model, the stabilization of the (311)B facet is due to the occupation of antisite complexes ($V_{Ga}Ga_{Sb}Te_{Sb}$) followed by the formation of surface reconstruction. The cross-sectional (110) plane view of the GaSb:Te epilayer after stain etching reveals that there are two boundaries separating the upper and lateral regions of the epilayer. Further, a few Te striations are found in the lateral region of the epilayer, but none are found in the upper region. It is attributed to the different growth mechanisms of the upper and lateral regions of the epilayer. The growth time dependence of the morphology of the GaSb:Te epilayer indicates that the (311)B facet is formed initially and becomes dominant after the epilayer growth time of 3 h. The cross-sectional SEM image after stain etching reveals that two downward (311)B facets are formed under two (111)A facets and there are no Te striations in the lateral region due to the facet growth front.

ACKNOWLEDGMENTS

The authors would like to thank Professor A. Tanaka and H. Katsuno for providing plasma CVD facility, Professor M. Table and T. Mizuno for their help in photolithography. The authors are also thankful for financial support by grant-in-aid of the Scientific Research from the Japanese Ministry of Education, Science and Culture [Kiban(B) No. 14350164]. One of the authors (G.Z.) acknowledges financial support from the Japanese Ministry of Education, Culture, Sports, Science and Technology.

[1]P. Campbell and M. A. Green, J. Appl. Phys. **62**, 243 (1987).
[2]A. Wang, J. Zhao, and M. A. Green, Appl. Phys. Lett. **57**, 602 (1990).
[3]J. Zhao, A. Wang, P. Altermatt, and M. A. Green, Appl. Phys. Lett. **66**, 3636 (1995).
[4]M. A. Green, J. Zhao, A. Wang, P. J. Reece, and M. Gal, Nature (London) **412**, 805 (2001).
[5]K. J. Weber, K. Catchpole, and A. W. Blakers, J. Cryst. Growth **186**, 369 (1998).
[6]R. S. Williams, M. J. Ashwin, J. H. Neave, and T. S. Jones, J. Cryst. Growth **227-228**, 56 (2001).
[7]P. S. Dutta and H. L. Bhat, J. Appl. Phys. **81**, 5821 (1997).
[8]G. Zhang, K. Balakrishnan, T. Koyama, M. Kumagawa, and Y. Hayakawa, J. Cryst. Growth **256**, 243 (2003).
[9]A. F. Witt, J. Electrochem. Soc. **114**, 298 (1967).
[10]M. Kumagawa, Y. Takabe, and Y. Hayakawa, Jpn. J. Appl. Phys., Part 1 **22**, 585 (1983).
[11]S. H. Lee, C. Y. Fetzer, G. B. Stringfellow, D. H. Lee, and T. Y. Seong, J. Appl. Phys. **85**, 3590 (1999).
[12]S. H. Lee and G. B. Stringfellow, Appl. Phys. Lett. **73**, 1703 (1998).
[13]R. C. Sangster, in *Compound Semiconductors*, edited by R. K. Willardson and H. L. Goering (Reinhold, London, 1962), Vol. 1, p. 241.
[14]Meng-Chyi Wu and Chi-Ching Chen, J. Appl. Phys. **73**, 8495 (1993).
[15]P. Gladkov, E. Monova, and J. Weber, Semicond. Sci. Technol. **12**, 1409 (1997).
[16]T. Nishinaga, Cryst. Prop. Prep. **31**, 92 (1991).
[17]Z. R. Zytkiewicz, D. Dobosz, and M. Pawlowska, Semicond. Sci. Technol. **14**, 465 (1999).
[18]S. Zhang and T. Nishinaga, Jpn. J. Appl. Phys., Part 1 **29**, 545 (1990).
[19]A. F. Witt, H. C. Gotos, M. Lichtensteiger, and C. J. Herman, J. Electrochem. Soc. **125**, 1832 (1978).